Relative predissociation rates of OH ($A\ ^2\Sigma^+$, $v'=3$) from combined cavity ring down—Laser-induced fluorescence measurements

J. J. L. Spaanjaars, J. J. ter Meulen, and G. Meijer

Molecular and Laser Physics, University of Nijmegen, P.O. Box 9010, 6500GL Nijmegen, The Netherlands

Relative predissociation rates of OH ($A\ ^2\Sigma^+$, $v'=3$) have been determined for N' up to 17 by simultaneously measuring laser-induced fluorescence excitation and cavity ring down absorption in the same experimental setup. The results are in overall agreement with calculated predissociation rates by Yarkony [J. Chem. Phys. **97**, 1838 (1992)], but show a stronger increase of the predissociation rate with increasing N'. The obtained values for the quantum yield can be used in the application of the laser-induced predissociative fluorescence detection technique in combustion diagnostics. © *1997 American Institute of Physics.* [S0021-9606(97)03631-3]

I. INTRODUCTION

Laser-induced predissociative fluorescence (LIPF) detection has been proposed as a possible technique to determine 2D temperature distributions in flames, plasmas, discharges, etc., at atmospheric pressure.[1] The method has been applied to OH, O_2, and H_2O in various combustion processes by exciting these molecules to the short lived predissociated states, $A\ ^2\Sigma^+$, $v'=3$, $B\ ^3\Sigma_u^-$, and $\widetilde{C}\ ^1B_1$, respectively. Because the lifetime of the excited state (<100 ps) is much shorter than the collisional time (typically 1 ns at atmospheric pressure), the problem of the collisional quenching can in principle be avoided, which facilitates the quantitative determination of temperature fields. Despite this advantage, the LIPF technique has thus far not been established as a reliable method for temperature measurements. This finds its origin in a number of problems, which, when not solved properly, may easily give rise to large errors in the derived temperatures. The most important problems are the collisional refill of the state from which the excitation takes place, the rotational dependence of the electronic transition moment, and the rotational dependence of the predissociation rates of the excited states. The effects of the replenishment of the initial state can be made negligibly small by reducing the laser power, which, however, also reduces the signal intensity. The rotational dependence of the transition moment can be determined from absorption measurements at a well-defined temperature, which is not easy to perform for OH. For the $A\ ^2\Sigma^+$, $v'=3 \leftarrow X\ ^2\Pi$, $v''=0$ transition only theoretical values are known thus far.[2] This paper discusses the determination of the relative predissociation rates of the rotational states in $v'=3$.

Experimental values for the predissociation lifetimes of OH ($A\ ^2\Sigma^+$, $v'=3$) have been reported by Gray and Farrow[3] and Heard *et al.*[4] Gray and Farrow obtained absolute values for the lifetime for N' up to 9 from linewidth measurements in an optical–optical double resonance experiment. Heard *et al.* determined relative predissociation rates for N' up to 14 in LIF measurements in a low pressure flame. Their values are in reasonable agreement with calculated values of Yarkony,[5] whereas the results of Gray and Farrow show some serious discrepancies with the theoretical

results. The experimental uncertainty of the data of Heard *et al.* varies between 10% and 20% and is largest for higher N' states. Since these states are most important for temperature determinations by LIPF this strongly affects the accuracy of the temperatures obtained. We therefore decided to perform an experiment in which precise values for the relative predissociation lifetimes are obtained from a simultaneous measurement of absorption and fluorescence in a combined cavity ring down (CRD)—laser-induced fluorescence (LIF) experiment. The ratio of the absorption to the fluorescence signals is a direct measure of the predissociation rate. Measurements could be performed for N' up to 17. The results can be used in LIPF diagnostics and form a test of the calculations by Yarkony.

II. BACKGROUND

After excitation to the $A\ ^2\Sigma^+$, $v'=3$ state the OH molecules will undergo one of three different processes, as indicated in Fig. 1. By far the largest fraction will dissociate due to a crossing of the $A\ ^2\Sigma^+$ state with the repulsive $^4\Sigma^-$ state. According to the calculations of Yarkony, the predissociation rate increases strongly with the rotational quantum number N', ranging from 4.6×10^9 s^{-1} for $N'=0$ to 2.3×10^{10} s^{-1} for $N'=14$.[5] For higher rotational levels the repulsive $^2\Sigma^-$ and $^4\Pi$ states (not shown in Fig. 1) also come into play. Instead of dissociation, some of the excited molecules undergo a collision induced transition to either the electronic ground state (nonradiative decay) or to another rovibrational state within $A\ ^2\Sigma^+$, which may be followed by radiative decay to the $X\ ^2\Pi$ state. The former process is called collisional quenching. For both processes the collision rate essentially depends on the composition of the gas and the temperature. In contrast to the $A\ ^2\Sigma^+$, $v'=0$ and 1 states, there is no information available about the collision rates for the $v'=2$ and 3 states. Typical values for the collisional quenching rate for OH in $v'=0$ and $v'=1$ are of the order of 10^8–10^9 s^{-1} in flames at atmospheric pressure.[6,7] A minor fraction of nondissociating molecules will decay directly to the ground electronic state and emit fluorescence radiation. About 60% of these molecules decay to the $v''=2$ state and 40% to the $v''=3$ state. The radiative decay
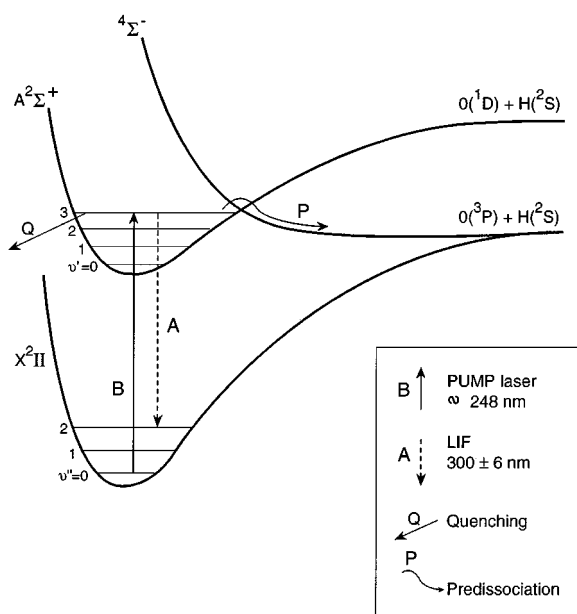
FIG. 1. The different decay processes of OH radicals after excitation to the $A\ ^2\Sigma^+$, $v'=3$ state.

rate ranges from 1.2×10^6 s^{-1} for $N'=0$ to 1.0×10^6 s^{-1} for $N'=14$.[5] It should be noted that the nonradiative decay of the $v'=3$ state might be influenced by collision induced effects on the predissociation, for which, however, no evidence is found in literature. We assume that these effects are small and can be neglected within the present experimental accuracy.

The intensity of the total fluorescence radiation emitted after excitation from a state $|i\rangle$ in $X\ ^2\Pi$ to a state $\langle j|$ in $A\ ^2\Sigma^+$ is given by:

$$S_{ij}=c\Phi_j B_{ij}I_L f_i, \tag{1}$$

where c is a constant containing the OH density and the irradiated volume, B_{ij} is the Einstein absorption coefficient, I_L is the laser intensity, f_i is the number of OH molecules in the state $|i\rangle$, given by the Boltzmann factor, and Φ_j is the fluorescence quantum yield:

$$\Phi_j=\frac{A(N',J')}{A(N',J')+P(N',J')+Q(N',J')}. \tag{2}$$

Herein N' and J' are the quantum numbers for the nuclear end-over-end rotation and the total orbital angular momentum of the excited state $|j\rangle$, respectively, and A, P, and Q are the state dependent rates for the spontaneous emission, predissociation, and collisional quenching, respectively. It should be noted that the Boltzmann factor in Eq. (1) can be used only in the weak excitation regime where collisional refill of the initial state can be neglected. In the denominator of Eq. (2) the spontaneous emission rate is much smaller than the other terms and can be neglected. Except for the low N' states, the predissociation rate is one to two orders of magnitude larger than the quenching rate, and Φ_j can be approximated by:

$$\Phi_j=\frac{A(N',J')}{P(N',J')}. \tag{3}$$

Not included in the expression for Φ_j is the fluorescence emitted from other v' states which are populated by collision induced vibrational energy transfer (VET) within the $A\ ^2\Sigma^+$ state from the $v'=3$ level. It can be shown that this contribution causes an increase of the quantum yield by a factor:

$$1+\sum_{v,N,J}\frac{A(v,N,J)}{A(v'=3,N',J')}\cdot\frac{R(v'=3,N',J'\to v,N,J)}{Q(v,N,J)}, \tag{4}$$

where $R(v'=3,N',J'\to v,N,J)$ is the rate of the collision induced transition from the excited $v'=3$ state to the state (v,N,J). Rotational energy transfer within the $v'=3$ state does not have to be taken into account; in this case the quenching rate $Q(v,N,J)$ in the denominator has to be replaced by the much larger predissociation rate $P(N,J)$, which makes this contribution negligibly small. In the present experiment a transmission filter is used which blocks all relatively strong transitions from states other than $v'=3$, with the exception of a fraction of the $v'=2\to v''=1$ band (see later). Therefore we decided to neglect the extra factor (4) in the quantum yield. Due to the partly observed $2\to1$ band an error will be introduced, which will be small if the rotational dependence of the VET is weak. The observed fluorescence is a fraction of S_{ij}, depending on the solid angle of the optics involved, the quantum efficiency of the detector, and the transmission of the filter in front of the detector.

Temperature determinations by the LIPF technique are based on the simultaneous measurement of two fluorescence signals from molecules in different initial states $|i\rangle$ and $|i'\rangle$. From the Boltzmann distribution and the ratio of the fluorescence signals S_{ij} and $S_{i'j'}$ the temperature is obtained:

$$T=\frac{(E_{i'}-E_i)}{k}\ln\left(c'\cdot\frac{S_{i'j'}}{S_{ij}}\cdot\frac{\Phi_j}{\Phi_{j'}}\cdot\frac{B_{ij}}{B_{i'j'}}\cdot\frac{g_i}{g_{i'}}\right), \tag{5}$$

where g_i and $g_{i'}$ are the degeneracies of the states $|i\rangle$ and $|i'\rangle$, respectively, and c' is a constant containing the difference of the experimental conditions for the two excitation and fluorescence processes. Since the accuracy of the temperature determination is inversely proportional to the energy difference $E_{i'}-E_i$, it is important to excite molecules in rotational states as far apart as possible. This also requires knowledge of the relative quantum yields for high N' states, for which we now report values for N' up to 17. In case the fluorescence is observed from an area along a line, Eq. (1) has to be modified into:

$$S_{ij}=c'B_{ij}\int\Phi_j I_L N_i(x)dx, \tag{6}$$

where the integration has to be performed over the length of the observation region, $N_i(x)$ is the local density of molecules in state $|i\rangle$, and c' is a constant. The quantum yield in principle depends on x via the collision rate Q. In the present experiment a flat flame burner is used with a constant tem-
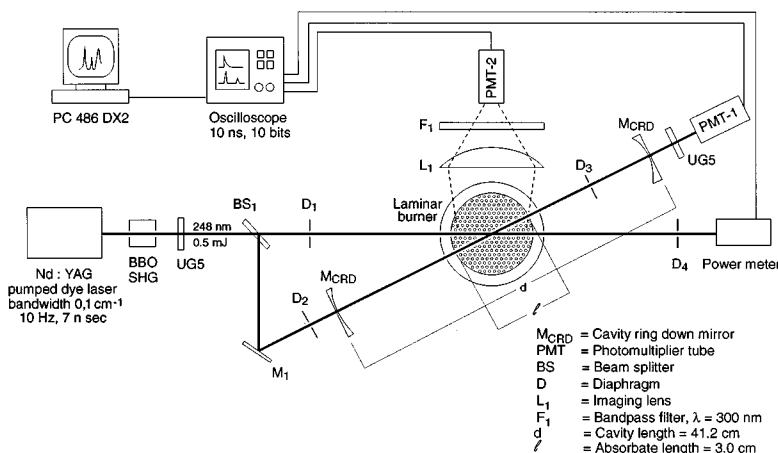
FIG. 2. Scheme of the experimental setup.

perature and species distribution along the laser beam direction over nearly the total area of the burner plate. Moreover, for the $v'=3$ state, the influence of Q on the quantum yield is small, and consequently Φ_j can be assumed to be constant over the path length. When absorption of the laser radiation is small Eq. (6) can be written as:

$$S_{ij} = c' \Phi_j B_{ij} I_L \int N_i(x) dx. \qquad (7)$$

In the present experiment the relative quantum yields are determined by a simultaneous measurement of fluorescence and absorption. Hereto the laser beam is split into two beams, one of which, with intensity I_L, is used for fluorescence excitation, and the other one, with intensity $I_{L'}$, for the absorption measurement in a CRD set up. In the CRD experiment the cavity decay time is measured, which is determined by the reflectivity of the cavity mirrors and the absorption of the molecules inside the cavity.[8] From the decay time and the known mirror reflectivity the absorption signal is obtained:

$$P_{ij} = \alpha B_{ij} \int N_i(x) dx, \qquad (8)$$

where α is a constant. In the experiment care is taken that the line integrated density is the same for both the fluorescence and absorption measurement. In this case division of the fluorescence signal of Eq. (7) by the absorption signal of Eq. (8) gives the quantum yield:

$$\frac{S'_{ij}}{P_{ij}} = \beta \Phi_j, \qquad (9)$$

where $S'_{ij} = S_{ij}/I_L$, the fluorescence signal normalized with respect to the laser power, and β is a constant factor, which in principle can be determined from the experimental conditions if the OH density is known.

III. EXPERIMENT

A scheme of the experimental setup is shown in Fig. 2. The OH molecules are produced in the laminar CH_4/air flame of a premixed adiabatically stabilized flat flame burner.[9] The circular burner plate has a diameter of 30 mm and thickness of 2.0 mm. The plate is perforated with a hexagonal pattern of approximately 2800 holes of 0.5-mm diameter and 0.7-mm pitch. The flow velocity and gas mixture is regulated by mass flow controllers (MFC) in such a way that no temperature gradient exists across the burner plate, which is a condition for adiabatic burning. This condition is controlled by five thermocouples in the burner plate. In the present experiment, the MFC setting is such that the flame is stabilized in a stoichiometric composition, with a flame velocity of 28 cm/s. LIF measurements show that in this situation the OH density distribution in a horizontal plane is homogeneous over about 90% of the cross sectional area of the flame. In a plane at about 8 mm above the burner plate the molecules are excited by 248-nm radiation from a frequency doubled Nd:YAG pumped dye laser (Quantel TDL 50). The laser beam is split into a low intensity beam which is deflected toward the cavity of the CRD setup and a beam of relatively high intensity for the fluorescence measurements. The intensity of the CRD beam should be kept low in order to allow for running the photomultiplier tube in an optimal linear power range. The intensity of the LIF beam is in all cases lower than 5.6 MW/cm^2 cm^{-1} (pulse energy≤5 mJ, beam diameter 3 mm, pulse duration 7 ns, bandwidth 0.18 cm^{-1}), in order to prevent sizeable collisional replenishment effects in the ground state.[10] The two beams cross each other in the center of the flame under an angle of about 35°. Although the beam paths are different, it can be assumed that due to the cylindrical symmetry of the burner the temperature and density distributions along the two paths are equal. Care has to be taken to prevent interference of both processes. Without proper shielding of the CRD circuit the Raman and Rayleigh scattering, evoked by the high intensity LIF beam, will cause a signal on the CRD detector even when blocking the CRD beam. By reducing the solid angle of the LIF beam toward both CRD mirrors, an effective reduction of this interference to less than 1% of the typical CRD signal can be obtained.

The fluorescence from OH molecules over the full length

of the burner plate is imaged onto the 10-mm photocathode of a photomultiplier tube by a set of quartz lenses. In front of the photomultiplier a Schott UG 11 filter is mounted in combination with a special band pass filter with a bandwidth of ± 7.5 nm around 300.0 nm. This filter transmits mainly the $v'=3 \rightarrow v''=2$ band and part of the $2 \rightarrow 1$ band. Both bands have about the same transition strength. In addition some very weak $1 \rightarrow 0$ lines are transmitted, as well as a few lines of the strong $0 \rightarrow 0$ band at the low frequency edge of the filter.

The ringing cavity for the absorption measurements consists of two highly reflecting mirrors in an optically stable setup. The distance between the mirrors is 41.2 cm, and the radius of curvature 25 cm. The reflectivity of the mirrors is determined in the same setup without burner. In this case a decay time (see below) of $\tau = 276$ ns is found, corresponding to a reflectivity of $R = 99.5\%$ at 247 nm. The laser pulse with an energy of typically 150 nJ is reflected back and forth between the two mirrors. The time dependence of the transmitted laser pulse energy is detected by a photomultiplier tube (PMT) operating in the linear regime. To reduce the continuous background signal caused by the flame front, a special narrow band pass filter (Schott, $\lambda = 253 \pm 20$ nm) is mounted in front of the PMT. Care has to be taken to position the PMT close to the outcoupling mirror of the cavity to ensure that all cavity modes are detected with equal probability. The combination of a wide linear range PMT and a fast high dynamic range digitizer is crucial for accurate determination of the absorption signal. In the present experiment a 10 bit, 100 M samples digital oscilloscope (LeCroy 9430) was applied. The burner is mounted in the center of the cavity.

In the ideal case the CRD signal shows an exponential decrease given by the decay time:

$$\tau = \frac{L}{c(|\ln R| + \sigma \int N(x)dx)}, \tag{10}$$

where c is the velocity of light, L the cavity length, R the reflectivity of the mirrors, and σ the absorption cross section. The integration is over the full length of the cavity, but in the present experiment can be limited to the path length above the burner, since the density of OH molecules outside the flame is negligibly small. Jongma et al.[8] have shown that due to either a too strong absorption or a too large laser bandwidth, the measured transient can deviate from an exponential curve. In this experiment, for each absorption line the measured CRD signal was checked on exponential behaviour. In all cases an exponential decay up to $t = 3.5\tau$ could be demonstrated. In the presence of the flame, absorption losses occur due to Rayleigh scattering and broadband absorption by hot oxygen, causing a decrease of the decay time from 276 ns to about 70 ns. On the strongest OH absorptions the decay time further decreases down to 50 ns.

Together with the signal from a power meter (fast diode) the PMT signals are fed to the digital oscilloscope, which is triggered by the laser. All signals are fed to a PC operating with specially designed software for data storage and deter-
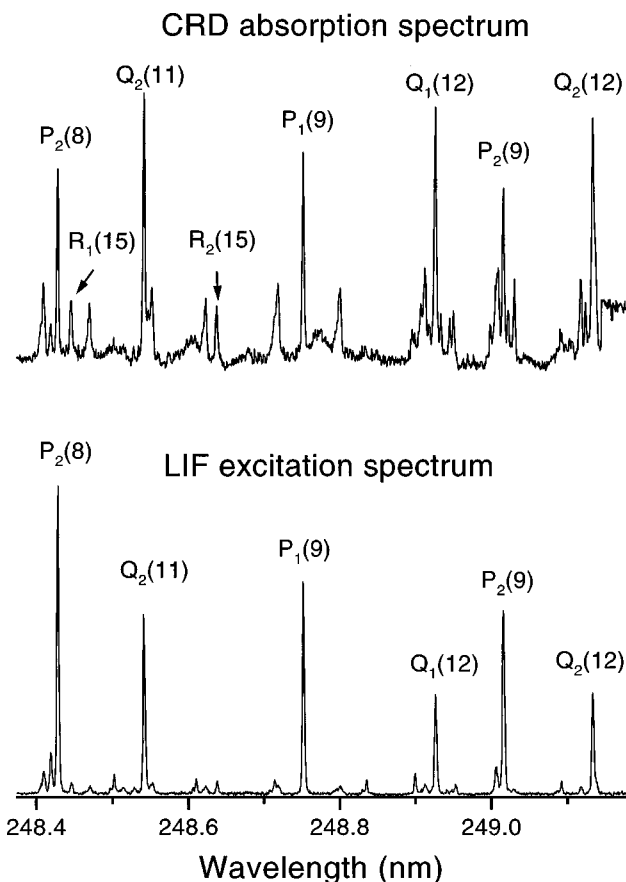

FIG. 3. Part of the $A\,^2\Sigma^+$, $v'=3 \leftarrow X\,^2\Pi$, $v''=0$ spectrum of OH, measured simultaneously by CRD and LIF. The differences in relative intensity due to the rotational dependence of the predissociation rate are clearly visible.

mination of decay times by means of fitting algorithms.[8] In all measurements each data point consists of a sampling of the CRD or LIF signal over 25 laser pulses.

IV. RESULTS

Several wavelength scans have been made in the range from 245 nm to 253 nm. A typical result is shown in Fig. 3. In the upper part of the figure the CRD absorption spectrum ($\propto 1/\tau$) is depicted, whereas the simultaneously measured LIF spectrum is shown in the lower part. A first inspection of the two spectra reveals a large difference in relative intensities. This is due to the strong rotational dependence of the predissociation in the $v'=3$ state, which causes a decreasing quantum yield for higher N' states. Whereas the intensities in the absorption spectrum increase with N'', which reflects the Boltzmann distribution peaking around $N''=12$, the fluorescence signal is strongly decreasing. In Fig. 3 the transitions to $N'=16$, which is the highest but one rotational state in $v'=3$ considered in the present work, are still clearly observable. In addition to the OH (A, $v'=3 \leftarrow X$, $v''=0$) lines, weaker lines are also observed in the absorption spectrum, which can be assigned to the Herzberg I band of O_2 ($A\,^3\Sigma_u^+$, $v'=9 \leftarrow X\,^3\Sigma_g^-$, $v''=0$).[11] A closer view of these O_2 lines is given in Fig. 4. It is mainly the oxygen in the
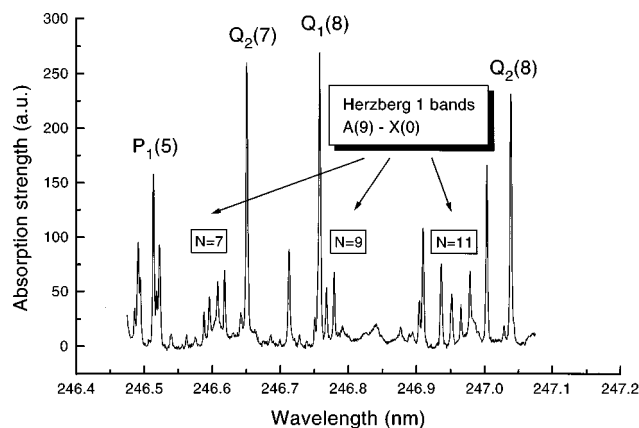
FIG. 4. Part of the CRD spectrum of OH ($A\ ^2\Sigma^+$, $v'=3\leftarrow X\ ^2\Pi$, $v''=0$) showing the Herzberg I bands of O_2.
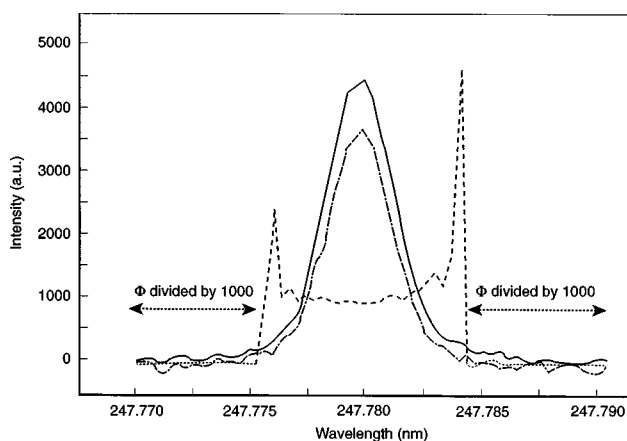

FIG. 5. The flat line shape of Φ for the $Q_1(10)$ transition as obtained by a point-by-point division of the normalized LIF signal (solid line) by the CRD signal (dashed-dotted line). The noise in the far outer wings is caused by the division of two nearly zero signals and is not relevant for the data reduction.

ambient air outside the flame which contributes to these signals. The presence of the Herzberg lines enabled us to determine the bandwidth of the laser by removing the flame so that temperature effects could be eliminated. Knowledge of the laser bandwidth is required in order to eliminate the interfering O_2 lines from the measured spectra. In addition to the Herzberg band, lines belonging to the Schumann–Runge band of O_2 ($B\ ^3\Sigma_u^-$, $v'=0,1,2\leftarrow X\ ^3\Sigma_g^-$, $v''=6,7$) are also observed, due to hot O_2 in the flame.

The relative quantum yields Φ were determined for N' between 6 and 17 by measuring P_1, P_2, Q_1, Q_2, R_1, and R_2 transitions. From the P_1, Q_1, and R_1 transitions, the quantum yield for the upper ρ-doublet states of e-symmetry (F_1 states) was obtained, whereas the quantum yield for the lower ρ-doublet states of f-symmetry (F_2 states) was determined from the P_2, Q_2, and R_2 transitions. Each line was measured four times or more in slow scans, with at least 11 data points per linewidth. As the LIF and CRD signals are simultaneously measured, a simple point-by-point division of the normalized LIF signal by the CRD signal yields a flat line shape, as shown in Fig. 5. The height of the resulting signal is proportional to the quantum yield, according to Eq. (9). Interferences with O_2 cause deviations from the flat line shape. In those cases accurate simulations of the respective O_2 spectra were subtracted from the CRD spectra to correct for this interference. No data points are presented in which this correction did not lead to a nice flat shape of the quantum yield over the full width of the transition. Another correction involved the change of the background level of the CRD signal during a scan, due to the wavelength dependence of the reflectivity of the mirrors. Hereto the background level was subtracted by fitting it first to a linear function of the wavelength.

The obtained results for the relative quantum yields are presented in Table I. The experimental accuracy given in Table I ranges from 8% for low N' states to 20% for the highest N' states. The results are scaled to the value of 81.0×10^{-6} for the F_2, $N'=11$ state as calculated by Yarkony.[5] In Table I the predissociation rates are also given

as obtained by multiplying the quantum yields by the radiative lifetimes as given by Yarkony.[5]

V. DISCUSSION

In Fig. 6 the scaled values for the quantum yield are compared to the calculated results of Yarkony, showing the same strong decrease for increasing N'. As was found also by Yarkony, the predissociation rate is consistently larger for F_1 states. In previous work on SH, similar differences were observed between the predissociated ρ-doublet states of the $A\ ^2\Sigma^+$, $v'=0$ state.[12] Also in this case the predissociation is caused by a repulsive $^4\Sigma^-$ state. It was shown by Ubachs that the differences can be explained by the spin-orbit interaction of the $^2\Sigma^+$ state with the $^4\Sigma^-$ state, which is stronger for the F_1 states than for the F_2 states.[13] Figure 6 gives the impression that the present values for the quantum yield are

TABLE I. Quantum yields Φ and lifetimes τ of the $A\ ^2\Sigma^+$, $v'=3$, N' rotational states of OH. The quantum yields are scaled to the value of 81.0×10^{-6} for F_2, $N'=11$ as calculated by Yarkony (Ref. 5). The lifetimes are derived from the values for Φ using the calculated radiative decay rates of Yarkony (Ref. 5). The values for $N'=6$ and 8 are based on interpolation of Yarkony's results; for $N'\geq15$ no radiative decay rates are reported.

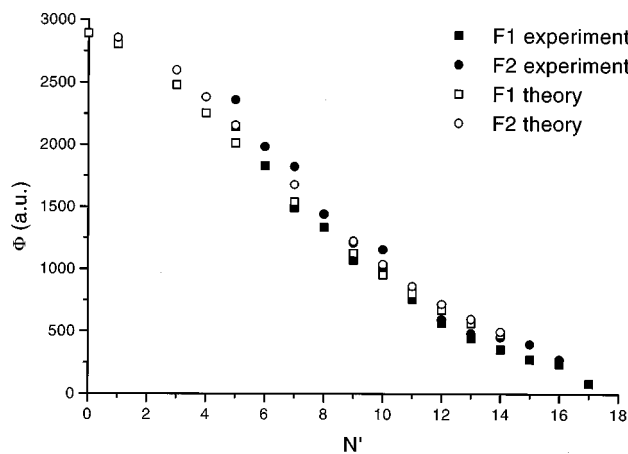| N'	$\Phi(F_1)$ $\times1.10^6$	$\Phi(F_2)$ $\times1.10^6$	$\tau(F_1)$ (ps)	$\tau(F_2)$ (ps)
5	202 ± 16	222 ± 18	167	154
6	173 ± 14	187 ± 15	144	156
7	159 ± 13	172 ± 15	134	145
8	126 ± 10	136 ± 11	107	116
9	101 ± 9	114 ± 10	87	99
10	96.2 ± 7.7	109 ± 9	85	96
11	67.7 ± 7.5	81.0 ± 8.1	61	73
12	51.4 ± 8.2	56.0 ± 5.6	47	51
13	40.0 ± 6.0	46.4 ± 7.0	38	44
14	30.3 ± 5.1	41.3 ± 5.0	29	40
15	26.0 ± 3.1	31.9 ± 6.4		
16	21.1 ± 3.8	21.7 ± 4.8		
17	13.0 ± 2.6			

FIG. 6. The measured quantum yield for OH in $A\ ^2\Sigma^+$, $v'=3$ as a function of the rotational quantum number N'. Also shown are the calculated values by Yarkony (Ref. 5). The experimental values are scaled to theory in F_2, $N'=11$.

larger than the calculated values for low N' states and smaller for high N' states, but this depends on the scaling point. Important for the application of these results in combustion diagnostics is the conclusion that the calculated values seem to overestimate the quantum yield for high N' states relative to the yield for low N' states up to about 50%. This discrepancy cannot be explained by the possible occurrence of collisional quenching of the excited state. Quenching would result in the opposite effect: a too small quantum yield for the lower N' states where the predissociation rate is smallest. Rotational energy transfer in the ground state would result in the observation of a too high quantum yield. However, at the applied laser intensities of <5.6 MW/cm^2 cm^{-1} the excitation efficiency is smaller than 5%, as calculated by using a value for the Einstein B coefficient of 11.7 s^{-1}/[W/cm^2 cm^{-1}] for the $Q_1(11)$ transition[2] and a pulse duration of 7 ns. It follows that RET effects are maximally of the order of a few percent, which cannot explain the observed discrepancy. It should be noted that also the results of Heard et al.[4] show a similar deviation with theory.

The values for the relative predissociation rates reported by Gray and Farrow[3] show large fluctuations with respect to the present data, far beyond the experimental accuracy. A comparison of the present results with the values reported by Heard et al. is made in Fig. 7(a) and 7(b) for F_1 and F_2 states, respectively. Also, in this comparison the values for Φ are scaled to match for $N'=11$, F_2. As can be seen from the figures the results are in qualitative agreement with respect to the overall N' dependence. For some of the quantum yields (particularly F_1, $N'=6$ and F_2, $N'=12$), however, deviations up to 30% are observed which are outside the range of the experimental accuracies. Noticeable also are the larger differences between the quantum yields for F_1 and F_2 states, not only in comparison to the present results, but also relative to the calculated values of Yarkony. Whereas in both Yarkony's work and the present measurements the differ-
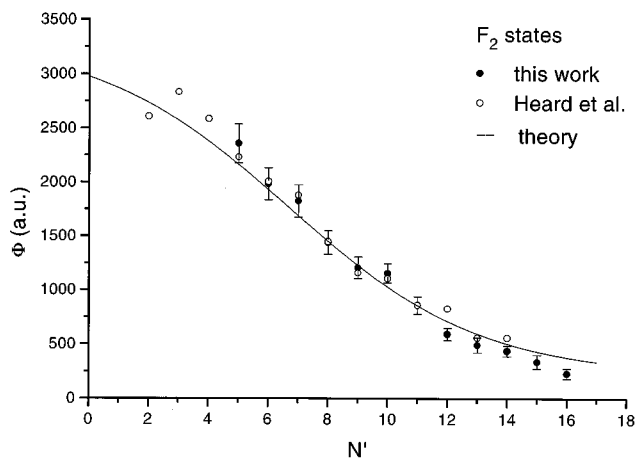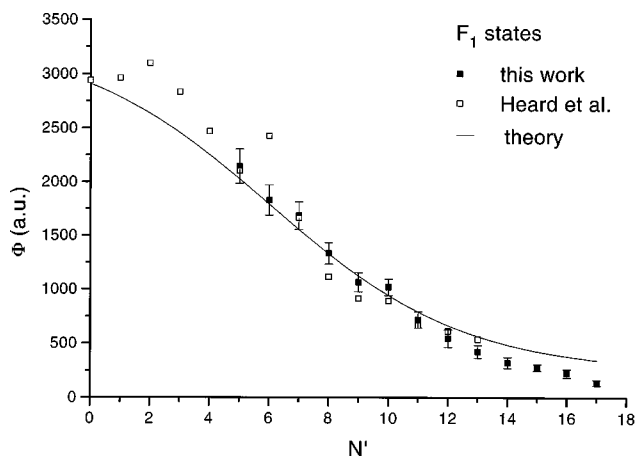

FIG. 7. A comparison of the present values for the relative quantum yield of OH ($A\ ^2\Sigma^+$, $v'=3$) with the results of Heard et al. (Ref. 4) for F_1 states (a) and F_2 states (b). The smooth curves connect the calculated values by Yarkony (Ref. 5). The values are scaled to each other in F_2, $N'=11$.

ences in Φ decrease with N', this is not the case for the results of Heard et al.

VI. CONCLUSIONS

The combination of LIF and CRD detection offers new possibilities to study predissociation effects. In this work the relative predissociation rates for OH ($A\ ^2\Sigma^+$, $v'=3$) were determined up to $N'=17$. Further improvement of the sensitivity by using mirrors with a higher reflectivity would allow the study of the predissociation of even higher rotational states. This is of particular interest because of the increasing importance of the repulsive $^2\Sigma^-$ and $^4\Pi$ states as dissociation channels. According to Yarkony the perturbation by these states is still negligible for the $v'=3$ predissociation. A larger influence of the $^2\Sigma^-$ and $^4\Pi$ states would, however, explain the relatively too low predissociation rates for the high N' states as calculated by Yarkony. This discrepancy, which is also shown by the results of Heard et al., may have important consequences for the application of the LIPF technique in combustion diagnostics. The accuracy of the temperature determination strongly improves with increasing energy range of the excited molecules, i.e., by measuring both

low and high N'' states, and consequently precise values for the quantum yield of high N' states are required. Experiments are in progress in which the present data are used for 2-D temperature determinations in laminar flames.

ACKNOWLEDGMENT

[1] P. Andresen, A. Bath, W. Gröger, H. W. Lülf, G. Meijer, and J. J. ter Meulen, Appl. Opt. **27**, 365–378 (1988).

[2] J. Luque and D. R. Crosley (private communication).

[3] J. A. Gray and R. L. Farrow, J. Chem. Phys. **95**, 7054 (1991).

[4] D. W. Heard, D. R. Crosley, J. B. Jeffries, G. P. Smith, and A. Hirano, J. Chem. Phys. **96**, 4366 (1992).

[5] D. R. Yarkony, J. Chem. Phys. **97**, 1838 (1992).

[6] P. M. Doherty and D. R. Crosley, Appl. Opt. **23**, 713 (1984).

[7] R. Kienle, A. Jörg, and K. Kohse-Höinghaus, Appl. Phys. B **56**, 249 (1993).

[8] R. T. Jongma, M. G. H. Boogaarts, I. Holleman, and G. Meijer, Rev. Sci. Instrum. **66**, 2821 (1995).

[9] A. van Maaren, D. S. Thung, and L. P. H. de Goey, Combust. Sci. Technol. **96**, 327 (1994).

[10] E. W. Rothe, Y. W. Gu, and G. P. Reck, Appl. Opt. **35**, 934 (1996).

[11] P. M. Borrell, P. Borrell, and D. A. Ramsay, Can. J. Phys. **64**, 721 (1986).

[12] W. Ubachs, J. J. ter Meulen, and A. Dymanus, Chem. Phys. Lett. **101**, 1 (1983); W. Ubachs and J. J. ter Meulen, J. Chem. Phys. **92**, 2121 (1990).

[13] W. Ubachs, thesis, University of Nijmegen, The Netherlands (1986).